Effectiveness of local methane and hydrogen injection into the scrape-off layer of W7-X by means of the Multi-Purpose Manipulator

P. Drews[a,*], T. Dittmar[a], C. Killer[b], V. Winters[b], A. Kirschner[a], S. Brezinsek[a], S. Xu[a], E. Wang[a], M. Jakubowski[b], K. J. Brunner[b], J. Knauer[b], O. Grulke[b], D. Höschen[a], A. Knieps[a], D. Nicolai[a], O. Neubauer[a], G. Satheeswaran[a], M. Hirsch[b], U. Höfel[b], Y. Liang[a], and the W7-X Team[b]

[a] *Forschungszentrum Jülich GmbH, Institut für Energie- und Klimaforschung Plasmaphysik, Partner of the Trilateral Euregio Cluster (TEC), 52425 Jülich, Germany*
[b] *Max-Planck-Institut für Plasmaphysik,17491 Greifswald, Germany*

Abstract

The Multi-Purpose-Manipulator (MPM) situated at the outboard mid-plane is a versatile carrier system for diagnostic probes at Wendelstein 7-X (W7-X). It is able to probe into the last scrape-off (SOL) layer close to the last closed flux surface. The manipulator is also has the capability to puff gas for well-localized fueling/impurity seeding into SOL. In the previous operational campaign of OP 1.2a and 1.2b both hydrogen and methane were injected from the manipulator mounted probes. The effect of hydrogen puffing on the main plasma was observed to be much stronger than that of the methane puffing. This difference is related to the difference in ionization lengths between the two gas species. To support this assumption a puffing of a similar amount of methane and hydrogen was modelled with ERO.

Keywords: `W7-X, Multi-purpose Manipulator, Langmuir probes, plasma edge transport, gas puffing, ERO`
2020 MSC:

1. Introduction

Extrinsic impurity puffing plays an important role in both operation of a fusion device concerning the management of divertor heat loads and impurity transport studies. W7-X has a 5/5 edge island structure that can strongly affect the efficiency of the puffing concerning the gas species and the position relative to the edge islands. In this paper two cases of gas puffing are compared, hydrogen and methane. From this comparison a measure of the effectiveness of the gas puffing in the edge of W7-X with different gas species can be found. Furthermore in this paper the effect of the position of the puffing for methane and hydrogen is discussed. Three distinct areas of note are shown in figure 1, the far scrape-off layer characterized by short magnetic connection lengths (III), the island region with magnetic connection lengths ranging from $L_{\mathrm{C\,island}} \approx 300\,\mathrm{m}$ to infinite in the island center (II) and the confined region (I). The effect of the puffing on the plasma depends largely where the injected gas is ionized, this depends on the position of the gas injection and the neutral penetration depth of the species. This neutral penetration depth is affected by the gas species and the local plasma parameters at the injection site.

Impurities can be puffed downstream (near the divertor target plates) with the gas boxes of the helium beam [1] and upstream ablation of impurities with the laser blow-off system [2] is possible. A system for upstream gas puffing is the Multi-purpose manipulator (MPM). It was installed at W7-X as a carrier system for both diagnostic and material exposition probe heads [3]. The MPM gas injection system consists of an internal gas reservoir of about 2.5 L. From this reservoir a feed line of 6 m length and 6 mm diameter runs to the probe head interface. However,

*Corresponding author
Email address: `p.drews@fz-juelich.de` (P. Drews)

in this scenario the gas stream is only controlled by a pneumatic valve at the gas reservoir. The total amount of puffed gas is controlled by filling the gas reservoir of the MPM gas handling system to different pressures. In 1.2a the internal MPM gas reservoir is openend for a short time (250 and 500 ms for discharge #20171101.028 and #20171101.029 respectively) at $p_{\mathrm{prefill}} \approx 0.2\,\mathrm{bar}$ pressure and the gas flows freely to the nozzle at the MPM probe head.

For OP 1.2b (2018) an additional probe head for controlled gas puffing employing an internal reservoir and a piezo valve located directly in the head were used [4]. The gas pressure was set in the methane puffing experiments to $p_{\mathrm{prefill}} \approx 0.5\,\mathrm{bar}$.

The position of the puffing in the considered experiments is located in the far scrape off layer with short connection length (see figure 1). The distance to the region of longer connection length close to the edge island is about $\Delta R \approx 4\,\mathrm{cm}$. The penetration depth depends largely on the speed of the injected molecules, at the same temperature and pressure hydrogen will be faster and therefore, penetrate deeper than methane. The second factor are the different cross sections for reactions connected to the dissociation and ionization of the molecules. The methane-electron collision cross section [5] is roughly three times larger than the hydrogen-electron cross-section [6]. The ion-electron ionization scales linearly with the plasma density. Thus the penetration depth of hydrogen in the edge would be approximately two times smaller in an OP 1.2b plasma. Using the densities at the interface between the far and near scrape off layer at $R \approx 6.08\,\mathrm{m}$ from figure 3 of $n_{e-OP1.2a} \approx 2 \times 10^{18}\,\mathrm{m}^{-3}$ and $n_{e-OP1.2b} \approx 4 \times 10^{18}\,\mathrm{m}^{-3}$. Depending on the edge densities the penetration depth of hydrogen for ion-electron collisions is between $\lambda_{H_2} \approx 5 - 11\,\mathrm{cm}$ and $\lambda_{CH_4} \approx 0.5 - 1\,\mathrm{cm}$. Due to the longer ionization mean free path, a larger fraction of neutral hydrogen should penetrate into the region of long connection length as compared to methane. With an ionization length of less than 1 cm, it is expected that the majority of the methane partially ionizes and then is lost immediately in the region of short connection length.

The experimental scenarios for the hydrogen and methane injection were conducted in comparable conditions. The same probe puffing position was used ($R_{\mathrm{puffing}} = 6.11\,\mathrm{m}$ see figure 1) and both experiments were performed in the same magnetic standard configuration in purely ECR heated plasmas. However, the plasma densities were unfortunately not comparable since the hydrogen puffing experiments in the earlier 2017 campaign were conducted at rather low densities, while the methane injection experiments took place in the 2018 campaign after a boronization of W7-X [7], which allowed considerably higher plasma densities. In table 1 the considered discharges with the total amount of injected molecules are presented.

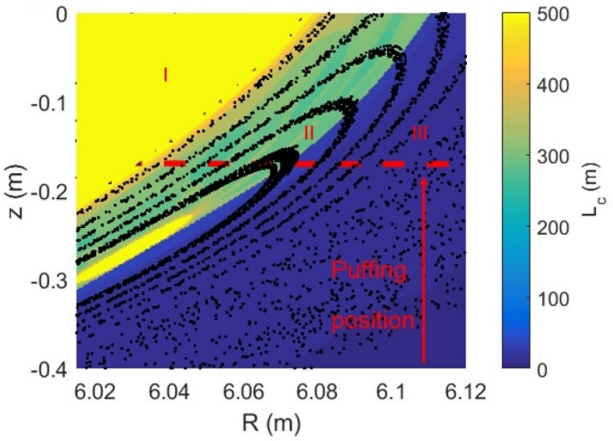

Figure 1: Cross section at the MPM position showing the connection length in standard configuration overlayed with the Poincaré plot. The red dashed line indicates the MPM path and the red arrow the puffing position of the hydrogen and methane injection (adapted from [4])

#	Gas-puffing	total amount of injected molecules
20171101.028	H_2	2.0 e21
20171101.029	H_2	3.6 e21
20180920.018	CH_4	1.2 e21
20180920.020	CH_4	1.4 e21
20180920.021	CH_4	1.4 e21

Table 1: Summary of the analyzed discharges

2. Observed effect of the puffing on the plasma

The injection of gas from the manipulator mounted probes into the plasma should yield in the first order two easily visible results on the main

plasma: an increase in density and a reduction of the plasma temperature. If the transport of the hydrogen and methane gases into the main plasma were the same, one would expect that for the same amount of molecules a larger effect on the electron density would be seen with methane. An important distinction has to be made concerning the plasma conditions of the hydrogen puffing in OP 1.2a and the methane puffing in OP 1.2b. The density in the edge region is expected to be higher in the latter case similar to the overal line integrated density. One has to assume that the difference of the edge densities correlates with the observed difference of the line integrated densities shown in figure 2, due to the lack of probe measurements. In the lower part of figure 3 measured edge densities and temperatures for both campaign parts are presented.

Figure 2 shows the time evolution of the electron density (a) measured with the interferometer and the electron temperature (b) as measured with the ECE system. For the hydrogen puffing a strong modification of the electron density and temperature is visible. A short delay of about $T_{\mathrm{delay}} \approx 0.1\,\mathrm{s}$ between the opening of the MPM gas valve and the observed density rise can be observed. The temperature recovers after the puff as the electron density decreases again. Discharge #20171101.028 has the valve open for 250 ms and 500 ms for discharge #20171101.029, this would yield approximately twice as many molecules injected in the latter. A slightly larger modification of electron density and temperature is observed, but the extend of the effect is difficult to assess, since the start of the puffing coincides with decrease of the plasma density and the larger hydrogen puff might just cause a higher observed baseline in the density measurements at $T \approx 1\,\mathrm{s}$. In the case of methane puffing both the electron temperature and the density show very little change. The density time trace of discharge # 20180920.021 with methane injection features slight bumps every 500 ms, which is caused by the blibs of the NBI system. In discharge # 20180920.020 and # 20180920.021 a small linear increase of the density is visible. Matching that, the electron temperature is decreasing slightly. The measurements show a visible modification of the temperature and density from hydrogen puffing but no or very little effect in the case methane.

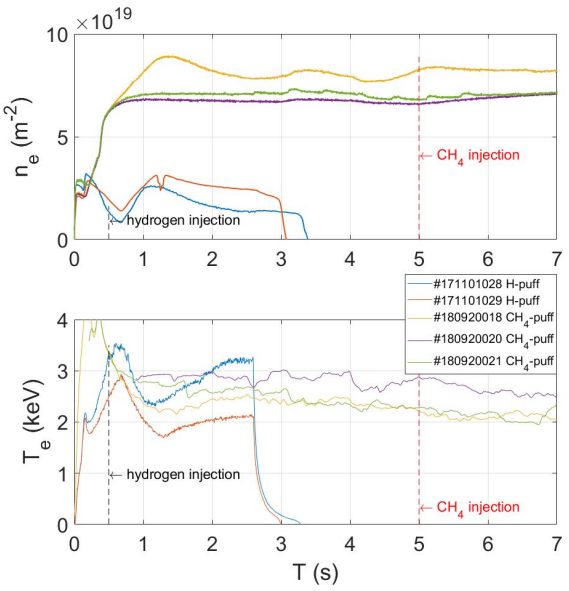

Figure 2: Upper figure: Line integrated densities for the hydrogen and methane puffing. Lower figure: Electron temperatures from channel #13 of the ECE system. The dashed line indicatse the beginning of the gas injection

3. Modelling of the methane puffing

The 3D Monte-Carlo code ERO [8] was employed to test the effectiveness of the methane and hydrogen puffing. A local plasma volume of $5 \times 10 \times 10\,\mathrm{cm}^3$ was used for the calculations. Radial electron temperature and density profiles from discharge #180814.045 measured with the MPM were used as a proxy for the plasma background (see figure 3), since the MPM had no probe measurements during the puffing. The molecules are injected into the plasma with a Maxwellian energy distribution around 0.05 eV and a cosine angular distribution. The upper part of figure 3 shows exemplarily the C^+ density resulting from CH_4 injection, integrated along the toroidal direction. The middle part of the figure summarizes modelled radial profiles (normalized to 1) of CH_4, CH and C^+ from CH_4 injection and H_2, H_2^+ and H^+ from H_2 injection. It is seen that the penetration length of injected CH_4 is significantly shorter than the one of injected H_2 molecules. The deeper penetration of the hydrogen for both the pure hydrogen puff and the hydrogen contained in the methane is evident. The still small density modification from the hydrogen contained in the methane cold be explained with the higher edge densities present during the ex-

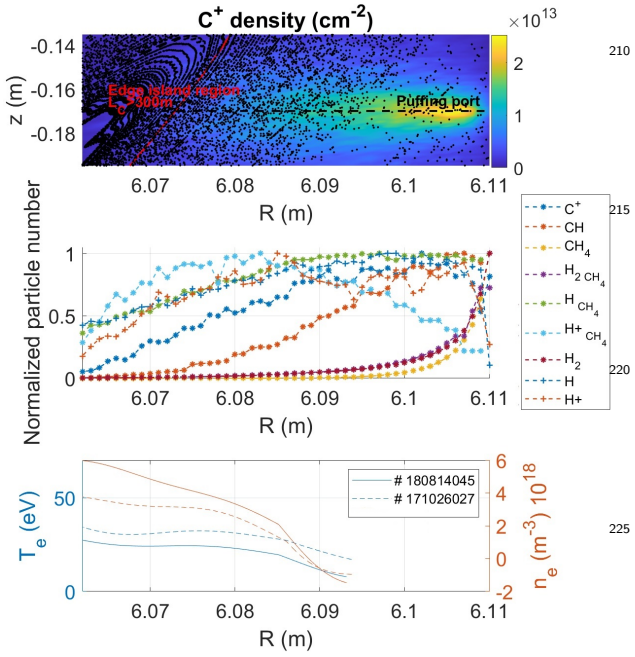

Figure 3: Upper figure: C^+ density calculated with ERO in front of the probe. Center figure: Normalized C^+, CH, CH_4, H_2, H and H^+ profiles from the methane puff and normalized H_2, H and H^+ profiles from the hydrogen puff. Lower figure: Temperature and density profile, used for the ERO model, measured with the MPM in discharge #180814.045 (line lines) and discharge #171026.027 (dashed lines) as a comparison for OP 1.2a.

periments of OP 1.2b. THE ERO calculation also yields, that about 36% of injected carbon and hydrogen species returns to the MPM in case of CH_4 injection, while only about 7% of injected H returns in case of H_2 injection. Altogether it can be concluded, that more particles (and also electrons) from a H_2 injection can reach the region of long connection lengths compared to a CH_4 injection.

4. Conclusion

The effectiveness of hydrogen and methane puffing from the manipulator was compared. While one would have expected a larger effect of the methane injected in similar quantities into the plasma than hydrogen, only the hydrogen puffing showed an actual effect on the plasma. This was explained with the comparatively short ionization depth of methane in the far scrape off layer region with short connection length. ERO was used to simulate puffing in the region of short connection length and showed that the methane has a considerably shorter penetration depth, at the same plasma parameters, than the injected hydrogen.

While the MPM system is able to puff in different regions in the plasma edge, the effectiveness strongly depends on the position of the puffing, the plasma parameters and the utilized gas species. It is necessary to fully accomodate these three parameters in the planning of gas puffing. The results suggest that the manipulator is suitable for the use of puffing into the island region, if the right positioning of the probe, in relation to the ionization depth and the intended effect on the plasma, is possible. Puffing of heavy gases into the edge islands region would necessitate a puffing system, with a Piezo valve, that can withstand the high heat loads during the puffing in the island region or the system used in first part of the campaign with a valve placed further down the gas puffing system and away from the nozzle.

5. Acknowledgements

This work has been carried out within the framework of the EUROfusion Consortium and has received funding from the Euratom research and training programme 2014-2018 and 2019-2020 under grant agreement No 633053. The views and opinions expressed herein do not necessarily reflect those of the European Commission.

The authors gratefully acknowledge the computing time granted by the JARA-HPC Vergabegremium and VSR commission on the supercomputer JURECA at Forschungszentrum Jülich.

References

[1] T. Barbui, The he/ne beam diagnostic for line-ratio spectroscopy inthe island divertor of wendelstein 7-x, Journal of Instrumentation 14 (2019) C07014 (2019). doi:https://doi.org/10.1088/1748-0221/14/07/C07014.

[2] T. Wegner, Design, capabilities, and first results of the new laser blow-off system on wendelstein 7-x, Review of Scientific Instruments 89 (2018) 073505 (2018). doi:https://doi.org/10.1063/1.5037543.

[3] D. Nicolai, A multi-purpose manipulator system for w7-x as user facility for plasma edge investigation, Fusion Engineering and Design 123 (2017) 960–964 (2017). doi:https://doi.org/10.1016/j.fusengdes.2017.03.013.

[4] P. Drews, Operation of probe heads on the multi-purpose-manipulator at w7-x in op 1.2a, Fusion Engineering and Design 146 (2019) 2353–2355 (2019). doi:https://doi.org/10.1016/j.fusengdes.2019.03.188.

[5] X. Liu, Analysis of electron impact ionization properties ofmethane, JOURNAL OF GEOPHYSICAL RESEARCH 111 (2006) A04303 (2006). doi:doi:10.1029/2005JA011454.

[6] W. Hu, Electron-impact-ionization cross section for the hydrogen atom, Physical REVIEW A 49 (1994) 989–991 (1994).

[7] S. Sereda, Impact of boronizations on impurity sources and performance in wendelstein 7-x, Nuclear Fusion 60 (2020) 086007 (2020). doi:https://doi.org/10.1088/1741-4326/ab937b.

[8] A. Kirschner, Simulation of the plasma-wall interaction in a tokamak with the monte carlo code ero-textor, Nuclear Fusion 40 (2000) 989–1001 (2000). doi:10.1088/0029-5515/40/5/311.